Pure P and S wave equations in transversely isotropic media

Alexey Stovas (NTNU, Norway), Tariq Alkhalifah (KAUST, Saudi Arabia) and Umair bin Waheed (KFUPM, Saudi Arabia)

Corresponding author: Alexey Stovas, 7491 S.P. Andersensvei, 15A, Trondheim Norway (alexey.stovas@ntnu.no)

Running head: Pure P and S wave equations

Abstract

Pure mode wave propagation is important for applications ranging from imaging to avoiding parameter tradeoff in waveform inversion. Although seismic anisotropy is an elastic phenomenon, pseudo-acoustic approximations are routinely used to avoid the high computational cost and difficulty in decoupling wave modes to obtain interpretable seismic images. However, such approximations may result in inaccuracies in characterizing anisotropic wave propagation. We propose new pure mode equations for P- and S-waves resulting in an artifact-free solution in transversely isotropic medium with a vertical symmetry axis. Our approximations are more accurate than other known approximations as they are not based on weak anisotropy assumptions. Therefore, the S-wave approximation can reproduce the group velocity triplications in strongly anisotropic media. The proposed approximations can be used for accurate modelling and imaging of pure P- and S-waves in transversely isotropic media.

Keyword: Anisotropy, Seismic theory, Wave propagation

This article has been accepted for publication and undergone full peer review but has not been through the copyediting, typesetting, pagination and proofreading process, which may lead to differences between this version and the Version of Record. Please cite this article as doi: 10.1111/1365-2478.13026.

Introduction

In anisotropic media, including the highly utilized transversely isotropic assumption, the P- and SV-waves are coupled, which prevents modelling for pure P- or SV- waves. Separate equations for different wave modes are important for many applications. However, to obtain such pure mode equations, we often resort to approximations. For P-waves, pure mode solutions are also convenient because they depend on fewer parameters. Typically, the parameter associated with the vertical shear wave velocity is excluded due to the low sensitivity of P-wave propagation to this parameter. The standard used approach, better known as acoustic approximation, is based on setting the vertical shear wave phase velocity to zero (Alkhalifah, 1998; 2000). Despite of its reasonable accuracy, the approximation suffers from shear wave artifacts (Grechka *et al*., 2004; Jin and Stovas, 2018; 2020). For the S-wave equations, we cannot exclude vertical P-wave phase velocity and all anisotropy parameters are needed.

Several approximations for the phase velocity of P- and SV-waves have been developed for transversely isotropic media with a vertical symmetry axis (VTI), i.e. separable P- and SV-wave equations. Most of them are based on approximations of the square root using various types of Pade approximations applied to the solution of the characteristic Christoffel equation (Dellinger *et al*., 1993; Schoenberg and de Hoop, 2000; Klie and Toro, 2001; Pestana *et al*., 2012; Schleicher and Costa, 2016). A very extensive review of phase velocity approximations can be found in Stopin (2001) and Fowler (2003). The general approach to velocity approximations is proposed in Stovas and Fomel (2019).

In this paper, we propose an entirely novel approach to derive separate equations for P- and SV-phase velocities in VTI media. The derived equations are tested using the well-known

benchmark model (Green Horn Shale) and compared with equations from Pestana *et al*. (2012).

Method

The parameters of our model are the stiffness coefficients $c_{11}, c_{33}, c_{55}, c_{66}$ and the anellipticity parameter η. In order to illustrate our method, we select the Green Horn Shale sample with the following parameters: $c_{11} = 14.47,\ c_{13} = 4.51,\ c_{33} = 9.57,\ c_{55} = 2.28$. The anellipticity parameter $\eta = 0.341$, which reflects strong anellipticity. The stiffness coefficient c_{13} is replaced by anellipticity parameter by using equation

$$\eta = \frac{(c_{11} - c_{55})(c_{33} - c_{55}) - (c_{13} + c_{55})^2}{2\left[(c_{33} - c_{55})c_{55} + (c_{13} + c_{55})^2\right]}. \quad (1)$$

Note the non-symmetric nature of anellipticity parameter (Sripanich and Fomel, 2015).

The characteristic equation in TI media, parameterized using the diagonal stiffness coefficients $c_{11}, c_{33}, c_{55}, c_{66}$ and the anelliptic parameter η, can be factorized into

$$F = F_{SH} F_{P-SV} = 0, \quad (2)$$

with

$$\begin{aligned} F_{SH} &= c_{66} n_1^2 + c_{44} n_3^2 - v^2, \\ F_{P-SV} &= \left(c_{11} n_1^2 + c_{55} n_3^2 - v^2\right)\left(c_{55} n_1^2 + c_{33} n_3^2 - v^2\right) - (c_{33} - c_{55})\left(\frac{c_{11}}{1+2\eta} - c_{55}\right) n_1^2 n_3^2, \end{aligned} \quad (3)$$

where v is the phase velocity and n_j, $j=1,2,3$ are the projections of the unit vector in phase domain.

The P-SV equation in (3) results in a quadratic formula for phase velocity squared,

$$F_{P-SV} = v^4 - Av^2 + B = 0, \qquad (4)$$

with coefficients given by invariants of P-SV block of Christoffel matrix,

$$\begin{aligned} A &= Tr\left(\mathbf{G}_{P-SV}\right) = \left(c_{11}+c_{55}\right)n_1^2 + \left(c_{33}+c_{55}\right)n_3^2, \\ B &= \det\left(\mathbf{G}_{P-SV}\right) = c_{11}c_{55}n_1^4 + \left(c_{33}c_{55} + c_{11}\frac{c_{55}+2c_{33}\eta}{1+2\eta}\right)n_1^2n_3^2 + c_{33}c_{55}n_3^4. \end{aligned} \qquad (5)$$

The 2x2 matrix $\mathbf{G}_{P-SV}$ is defined in Appendix A.

Exact roots of equation (4) are given by

$$\begin{aligned} v_{P,S}^2\left(n_1,n_3\right) = \frac{1}{2}\Bigg(& c_{11}n_1^2 + c_{33}n_3^2 + c_{55}\left(n_1^2+n_3^2\right) \\ & \pm \sqrt{\left[c_{11}n_1^2 + c_{33}n_3^2 - c_{55}\left(n_1^2+n_3^2\right)\right]^2 - \frac{8\eta c_{11}\left(c_{33}-c_{55}\right)n_1^2n_3^2}{\left(1+2\eta\right)}}\Bigg), \end{aligned} \qquad (6)$$

where signs + and – correspond to the P- and SV-waves, respectively.

Our goal is to define the coefficient $c_{55} = \tilde{\ }$ such that one of the roots of equation (4) will be zero, i.e. equation (4) reduces to

$\left(v^2 - \tilde{\ }\right.$ (7)

when one root $v^2 = \tilde{}$ controls P-wave propagation, and the other one is equal to zero and corresponds to SV-wave. The modified trace $\tilde{}$ consists of an elliptic part e and an anelliptic part a,

$$\tilde{} \qquad {}_3) + a(n_1, n_3), \qquad (8)$$

with

$$\begin{aligned} e &= c_{11}n_1^2 + c_{33}n_3^2, \\ a &= \left(n_1^2 + n_3^2\right)\tilde{} \end{aligned} \qquad (9)$$

Equation (7) reduces the rank of matrix $\mathbf{G}_{P-SV}$ to one, and the determinant of this matrix is zero. Solving equation $B = \det\left(\mathbf{G}_{P-SV}\right) = 0$ gives

$$\tilde{} \qquad = -\frac{2\eta c_{11}c_{33}n_1^2 n_3^2}{(1+2\eta)c_{33}n_3^2\left(n_1^2+n_3^2\right) + c_{11}n_1^2\left[n_1^2(1+2\eta)+n_3^2\right]}, \qquad (10)$$

and, therefore, the anelliptic component of $\tilde{}$ is given by

$$a(n_1, n_3) = -\frac{2\eta c_{11}c_{33}n_1^2 n_3^2\left(n_1^2+n_3^2\right)}{(1+2\eta)c_{33}n_3^2\left(n_1^2+n_3^2\right) + c_{11}n_1^2\left[n_1^2(1+2\eta)+n_3^2\right]}, \qquad (11)$$

Finally, the approximation for the P-wave phase velocity is given by the rational approximation,

$$v_P^2(n_1, n_3) = \tilde{} \qquad c_{33}n_3^2 - \frac{2\eta c_{11}c_{33}n_1^2 n_3^2\left(n_1^2+n_3^2\right)}{(1+2\eta)c_{33}n_3^2\left(n_1^2+n_3^2\right) + c_{11}n_1^2\left[n_1^2(1+2\eta)+n_3^2\right]}. \qquad (12)$$

Upon substituting the phase vector projections $n_1 = \sin\theta$ and $n_3 = \cos\theta$, equation (12) takes the form,

$$v_P^2(\theta) = c_{11}\sin^2\theta + c_{33}\cos^2\theta - \frac{2\eta c_{11}c_{33}\sin^2\theta\cos^2\theta}{(1+2\eta)c_{33}\cos^2\theta + c_{11}\sin^2\theta(1+2\eta\sin^2\theta)}. \quad (13)$$

The P-wave equation (13) is identical to a new acoustic approximation proposed in Xu *et al*. (2020).

The S-wave equation can easily be computed from coefficient A, equation (5) (by using Vieta's theorem, $v_P^2 + v_{SV}^2 = A$),

$$\begin{aligned} v_{SV}^2(n_1, n_2) &= A - v_P^2(n_1, n_2) \\ &= c_{55}(n_1^2 + n_3^2) + \frac{2\eta c_{11}c_{33}n_1^2n_3^2(n_1^2 + n_3^2)}{(1+2\eta)c_{33}n_3^2(n_1^2 + n_3^2) + c_{11}n_1^2\left[n_1^2(1+2\eta) + n_3^2\right]}, \end{aligned} \quad (14)$$

or in terms of the polar angle,

$$v_{SV}^2(\theta) = c_{55} + \frac{2\eta c_{11}c_{33}\sin^2\theta\cos^2\theta}{(1+2\eta)c_{33}\cos^2\theta + c_{11}\sin^2\theta(1+2\eta\sin^2\theta)}. \quad (15)$$

Since the idea behind our method is based on approximating the determinant of P-SV block of Christoffel matrix by eliminating SV-wave propagation, the SV-wave equation, on the other hand, is based on preserving the trace of P-SV block. It is worth illustrating using the exact and approximate (given by the product of P- and SV-wave phase velocities squared) determinants computed for Green Horn Shale (Figure 1). One can see that the approximation of the determinant, by introducing approximations for P- and SV-waves given respectively by equations (13) and (15), is very accurate for all phase angles.

The classic acoustic approximation (Alkhalifah, 1998; 2000) is based on setting the vertical shear wave phase velocity to zero. In our parameterization, it is equivalent to setting $c_{55} = 0$ in equations (4)-(5),

$$v^4 - \left(c_{11}n_1^2 + c_{33}n_3^2\right)v^2 + \frac{2\eta}{1+2\eta}c_{11}c_{33}n_1^2n_3^2 = 0, \qquad (16)$$

with well-known roots

$$\begin{aligned} v^2 &= \frac{1}{2}\left(c_{11}n_1^2 + c_{33}n_3^2 \pm \sqrt{\left(c_{11}n_1^2 + c_{33}n_3^2\right)^2 - \frac{8\eta}{1+2\eta}c_{11}c_{33}n_1^2n_3^2}\right) \\ &= \frac{1}{2}\left(c_{11}\sin^2\theta + c_{33}\cos^2\theta \pm \sqrt{\left(c_{11}\sin^2\theta + c_{33}\cos^2\theta\right)^2 - \frac{8\eta}{1+2\eta}c_{11}c_{33}\sin^2\theta\cos^2\theta}\right), \end{aligned} \qquad (17)$$

with sign notations being the same as for equation (6). The S-wave artifact can be obtained by selecting the minus sign in front of the square root.

To demonstrate the accuracy of our equations, we compare them with approximations from Pestana *et al*. (2012), which are based on the series approximations starting with the expansion of square root from equation (6). It results in

$$\begin{aligned} v_P^2(\theta) &= c_{11}\sin^2\theta + c_{33}\cos^2\theta - \frac{2\eta c_{11}c_{33}\sin^2\theta\cos^2\theta}{\left(1+2\eta\right)\left(c_{11}\sin^2\theta + c_{33}\cos^2\theta\right)}, \\ v_S^2(\theta) &= c_{55} + \frac{2\eta c_{11}c_{33}\sin^2\theta\cos^2\theta}{\left(1+2\eta\right)\left(c_{11}\sin^2\theta + c_{33}\cos^2\theta\right)}. \end{aligned} \qquad (18)$$

The accuracy of individual phase velocities (for P- and SV-waves) from our method (equations (13) and (15)) are compared with equations (18) for the Green Horn Shale in Figure 2. One can see that the proposed approximation performs better compared with the one from Pestana *et al*. (2012).

Slowness surface

An equation for the slowness surface can be easily computed from the equation for phase velocity by substitution $n_1 = p_1 v$, $n_3 = p_3 v$ (p_1 and p_3 are horizontal and vertical projections of the slowness vector, respectively) and eliminating phase velocity from equation. For P-wave, from equation (12), we obtain

$$F_P = -1 + c_{11}p_1^2 + c_{33}p_3^2 - \frac{2\eta c_{11}c_{33}p_1^2 p_3^2\left(p_1^2 + p_3^2\right)}{\left(1+2\eta\right)c_{33}p_3^2\left(p_1^2 + p_3^2\right) + c_{11}p_1^2\left[p_1^2\left(1+2\eta\right) + p_3^2\right]} = 0. \quad (19)$$

This is a third-order polynomial with respect to the squares of slowness projections,

$$b_3 p_3^6 + b_2 p_3^4 + b_1 p_3^2 + b_0 = 0, \quad (20)$$

where

$$\begin{aligned} b_3 &= c_{33}^2\left(1+2\eta\right), \\ b_2 &= -c_{33}\left\{1+2\eta - p_1^2\left[2c_{11} + c_{33}\left(1+2\eta\right)\right]\right\}, \\ b_1 &= -p_1^2\left\{c_{11} + c_{33}\left(1+2\eta\right) - c_{11}p_1^2\left[c_{11} + 2c_{33}\left(1+\eta\right)\right]\right\}, \\ b_0 &= -c_{11}\left(1+2\eta\right)p_1^4\left(1 - c_{11}p_1^2\right). \end{aligned} \quad (21)$$

All coefficients b_j, $j = 0,3$ are real functions of horizontal slowness which means that at least one root of equation (20) is a real function. The coefficient b_0 is always non-positive within the P-wave propagation range, $p_1^2 \le 1/c_{11}$, assuming $\eta \ge -1/2$. According to Postnikov (Postnikov, 1981) criterium, inequality $b_0 < 0$ implies that two roots of equation (20) have negative real parts and one root has a positive real part. There are two possibilities for these roots. They can be complex conjugate with negative real part or they can be real negative functions. Since the equation (20) is given in terms of the vertical slowness squared, we have

only one root that results in propagating P-wave and two roots which result in non-propagating waves.

The solution of equation (20) is shown in the Appendix B. When setting the anellipticity parameter $\eta = 0$, equation (20) reduces to

$$\left(p_1^2 + p_3^2\right)\left(-1 + c_{11}p_1^2 + c_{33}p_3^2\right)\left(c_{11}p_1^2 + c_{33}p_3^2\right) = 0, \quad (22)$$

with the P-wave elliptic factor $-1 + c_{11}p_1^2 + c_{33}p_3^2$.

The S-wave slowness surface can be computed in similar way,

$$F_{SV} = -1 + c_{55}\left(p_1^2 + p_3^2\right) + \frac{2\eta c_{11}c_{33}p_1^2 p_3^2\left(p_1^2 + p_3^2\right)}{\left(1+2\eta\right)c_{33}p_3^2\left(p_1^2 + p_3^2\right) + c_{11}p_1^2\left[p_1^2\left(1+2\eta\right) + p_3^2\right]} = 0, \quad (23)$$

that also leads to a cubic equation,

$$d_3 p_3^6 + d_2 p_3^4 + d_1 p_3^2 + d_0 = 0, \quad (24)$$

with coefficients

$$\begin{aligned}
d_3 &= c_{11}c_{33}\left(1+2\eta\right), \\
d_2 &= -c_{33}\left(1+2\eta\right) + p_1^2\left[c_{33}c_{55}\left(1+2\eta\right) + c_{11}\left(c_{55} + 2\eta c_{33}\right)\right], \\
d_1 &= -p_1^2\left[c_{11} + c_{33}\left(1+2\eta\right)\right] + p_1^4\left\{2c_{11}c_{33}\eta + c_{55}\left[\left(c_{33}\left(1+2\eta\right)\right) + 2c_{11}\left(1+\eta\right)\right]\right\}, \\
d_0 &= -c_{11}\left(1+2\eta\right)p_1^4\left(1 - c_{55}p_1^2\right).
\end{aligned} \quad (25)$$

One can see (see discussion after equation (21)) that within the SV-wave propagation range ($p_1^2 \le 1/c_{11}$) and condition $\eta \ge -1/2$, equation (24) results in one propagating SV-wave and two non-propagating waves.

When setting $\eta = 0$, equation (24) reduces to

$$\left(p_1^2+p_3^2\right)\left[-1+c_{55}\left(p_1^2+p_3^2\right)\right]\left(c_{11}p_1^2+c_{33}p_3^2\right)=0\,. \quad (26)$$

The P- and S-wave slowness surfaces computed from equations (20) and (24), respectively, are compared with the exact solutions in Figure 3. One can see that the accuracy of our approximations is very high for all wave modes.

Eikonal equation

Before computing eikonal equations for P- and SV-waves, we derive the group velocity surfaces from our approximations (13) and (15). To compute the group surfaces, the standard equations are still valid. The group velocity horizontal and vertical projections V_1 and V_3 are given by (see, for example, Brillouin (1960))

$$\begin{aligned} V_1 &= v\sin\theta+\frac{dv}{d\theta}\cos\theta, \\ V_3 &= v\cos\theta-\frac{dv}{d\theta}\sin\theta. \end{aligned} \quad (27)$$

The group velocity surfaces for the P- and SV-waves computed from proposed approximations (13) and (15), the Pestana *et al*. (2012) approximations (equations (18)) and exact equations (6) are shown in Figure 4. All P-wave group velocity surfaces are very similar, but for SV-wave, our approximation (15) is much better in reproducing triplication features (zoomed in Figure 5).

The P-wave eikonal equation derived from acoustic approximation is of fourth order in terms of the traveltime derivatives,

$$1-\left(\frac{\partial\tau}{\partial x}\right)^2 c_{11}-\left(\frac{\partial\tau}{\partial z}\right)^2 c_{33}+\frac{2\eta}{1+2\eta}\left(\frac{\partial\tau}{\partial x}\right)^2\left(\frac{\partial\tau}{\partial z}\right)^2 c_{11}c_{33}=0\,, \quad (28)$$

From equation (13), we obtain the new eikonal equation for P-wave,

$$\left[\left(\frac{\partial\tau}{\partial x}\right)^2+\left(\frac{\partial\tau}{\partial z}\right)^2\right]\left[c_{11}\left(\frac{\partial\tau}{\partial x}\right)^2+c_{33}\left(\frac{\partial\tau}{\partial z}\right)^2\right]\left[1-c_{11}\left(\frac{\partial\tau}{\partial x}\right)^2-c_{33}\left(\frac{\partial\tau}{\partial z}\right)^2\right]$$
$$+2\eta\left\{c_{11}\left(\frac{\partial\tau}{\partial x}\right)^4\left[1-c_{11}\left(\frac{\partial\tau}{\partial x}\right)^2-c_{33}\left(\frac{\partial\tau}{\partial z}\right)^2\right]+c_{33}\left(\frac{\partial\tau}{\partial z}\right)^2\left[\left(\frac{\partial\tau}{\partial x}\right)^2+\left(\frac{\partial\tau}{\partial z}\right)^2\right]\left[1-c_{33}\left(\frac{\partial\tau}{\partial z}\right)^2\right]\right\}=0. \tag{29}$$

The new SV-wave eikonal equation derived from equation (15) takes the form,

$$\left[\left(\frac{\partial\tau}{\partial x}\right)^2+\left(\frac{\partial\tau}{\partial z}\right)^2\right]\left[c_{11}\left(\frac{\partial\tau}{\partial x}\right)^2+c_{33}\left(\frac{\partial\tau}{\partial z}\right)^2\right]\left\{1-c_{55}\left[\left(\frac{\partial\tau}{\partial x}\right)^2+\left(\frac{\partial\tau}{\partial z}\right)^2\right]\right\}$$
$$+2\eta\left\{c_{33}\left(\frac{\partial\tau}{\partial z}\right)^2\left[1-c_{55}\left[\left(\frac{\partial\tau}{\partial x}\right)^2+\left(\frac{\partial\tau}{\partial z}\right)^2\right]\right]\right.$$
$$\left.-c_{11}\left(\frac{\partial\tau}{\partial x}\right)^2\left\{-\left(\frac{\partial\tau}{\partial x}\right)^2\left[1-c_{55}\left[\left(\frac{\partial\tau}{\partial x}\right)^2+\left(\frac{\partial\tau}{\partial z}\right)^2\right]\right]\right\}+c_{33}\left(\frac{\partial\tau}{\partial z}\right)^2\left[\left(\frac{\partial\tau}{\partial x}\right)^2+\left(\frac{\partial\tau}{\partial z}\right)^2\right]\right\}=0. \tag{30}$$

If $\eta=0$, equations (29) and (30) are respectively reduced to

$$\left[\left(\frac{\partial\tau}{\partial x}\right)^2+\left(\frac{\partial\tau}{\partial z}\right)^2\right]\left[c_{11}\left(\frac{\partial\tau}{\partial x}\right)^2+c_{33}\left(\frac{\partial\tau}{\partial z}\right)^2\right]\left[1-c_{11}\left(\frac{\partial\tau}{\partial x}\right)^2-c_{33}\left(\frac{\partial\tau}{\partial z}\right)^2\right]=0,$$
$$\left[\left(\frac{\partial\tau}{\partial x}\right)^2+\left(\frac{\partial\tau}{\partial z}\right)^2\right]\left[c_{11}\left(\frac{\partial\tau}{\partial x}\right)^2+c_{33}\left(\frac{\partial\tau}{\partial z}\right)^2\right]\left[1-c_{55}\left(\left(\frac{\partial\tau}{\partial x}\right)^2+\left(\frac{\partial\tau}{\partial z}\right)^2\right)\right]=0. \tag{31}$$

Discussion

From equations (7) and (8), one can see that the proposed phase velocity approximations are based on approximating $\tilde{\epsilon}$ or the anelliptic part of the P-wave phase velocity using the rational approximation. This approximation is based on setting the determinant of the P-SV block of the Christoffel matrix to zero, which guarantees we have only one propagating wave

mode supported by the developed equation. The same idea is adopted in developing the S-wave equation, the same "anelliptic" part is added to the "elliptic" part of the S-wave phase equation but with a different sign in order to preserve the trace of the P-SV block of the Christoffel equation. It is known that SV-wave anisotropy is coupled with P-wave anellipticity (Fowler, 2003). Obviously, the derived equations do not correspond to any physical medium but allow us to perform pure-mode wave propagation with sufficient accuracy. Note that the accuracy of both the P- and SV-wave equations is the same. The reason why the relative error in the SV-wave approximation is larger is because of the fact that the magnitude of the SV-wave velocity is smaller compared to the P-wave velocity.

To use the developed equations for wavefield modelling, we can define the dispersion relation (see, for example, Alkhalifah (1998)). For P- and SV-waves, the dispersion relation can be computed respectively from equations (13) and (15),

$$\omega^2 = f\left(k_x,k_z\right) = c_{11}k_x^2 + c_{33}k_z^2 - \frac{2\eta c_{11}c_{33}k_x^2k_z^2\left(k_x^2+k_z^2\right)}{c_{33}\left(1+2\eta\right)k_z^2\left(k_x^2+k_z^2\right)+c_{11}k_x^2\left[k_x^2\left(1+2\eta\right)+k_z^2\right]}, \quad (32)$$

$$\omega^2 = f\left(k_x,k_z\right) = \left(k_x^2+k_z^2\right)\left\{c_{55} + \frac{2\eta c_{11}c_{33}k_x^2k_z^2}{c_{33}\left(1+2\eta\right)k_z^2\left(k_x^2+k_z^2\right)+c_{11}k_x^2\left[k_x^2\left(1+2\eta\right)+k_z^2\right]}\right\}. \quad (33)$$

The corresponding wave equation in the time-wavenumber domain can be obtained from equations (32) or (33) by

$$\frac{\partial^2 P\left(t,k_x,k_z\right)}{\partial t^2} = -f\left(k_x,k_z\right)P\left(t,k_x,k_z\right), \quad (34)$$

where $P\left(t,k_x,k_z\right)$ is the wavefield defined in time-wavenumber domain.

Conclusions

We derive the new separate equations for P- and SV-waves in transversely isotropic media. The P-wave equation is computed by eliminating the SV-waves for all directions of propagation. By using the P-wave approximation, the SV-wave equation is computed by preserving the trace of the P-SV block of the Christoffel matrix. The proposed approximations are tested against existing approximations for the Green Horn Shale model and exhibit superior accuracy.

Acknowledgements

Alexey Stovas acknowledges the GAMES project at NTNU. We would like to acknowledge Associate Editor Yuriy Ivanov and reviewers Igor Ravve and Pavel Golikov for very instructive comments.

Appendix A

Decoupling of P-SV and SH waves

The Christoffel matrix for a VTI medium with a vertical symmetry axis has the following form,

$$\mathbf{G}=\begin{pmatrix} c_{11}n_1^2+c_{55}n_3^2 & 0 & \sqrt{(c_{33}-c_{55})\left(\frac{c_{11}}{1+2\eta}-c_{55}\right)}n_1n_3 \\ 0 & c_{66}n_1^2+c_{44}n_3^2 & 0 \\ \sqrt{(c_{33}-c_{55})\left(\frac{c_{11}}{1+2\eta}-c_{55}\right)}n_1n_3 & 0 & c_{55}n_1^2+c_{33}n_3^2 \end{pmatrix}. \quad \text{(A-1)}$$

It worth noting that the wave propagation is restricted to the (n_1, n_3) plane due to cylindrical symmetry. One can see that the SH wave is decoupled from P-SV waves. The P-SV block of Christoffel matrix can be obtained by deleting the second raw and second column of matrix (A-1)

$$\mathbf{G}_{P-SV} = \begin{pmatrix} c_{11}n_1^2 + c_{55}n_3^2 & \sqrt{(c_{33}-c_{55})\left(\frac{c_{11}}{1+2\eta}-c_{55}\right)}n_1 n_3 \\ \sqrt{(c_{33}-c_{55})\left(\frac{c_{11}}{1+2\eta}-c_{55}\right)}n_1 n_3 & c_{55}n_1^2 + c_{33}n_3^2 \end{pmatrix}. \quad \text{(A-2)}$$

Appendix B

Solving the cubic equation

To solve the cubic equation for the vertical slowness squared (20),

$$b_3 p_3^6 + b_2 p_3^4 + b_1 p_3^2 + b_0 = 0, \qquad \text{(B-1)}$$

we need to compute

$$\begin{aligned} r &= \frac{3b_1 b_3 - b_2^2}{3b_3^2}, \\ q &= \frac{2b_2^3 - 9b_1 b_2 b_3 + 27b_3^2 b_0}{27b_3^3}, \qquad \text{(B-2)} \\ D &= 4r^3 + 27q^2. \end{aligned}$$

Since $D \geq 0$, we can use Cardano's formula,

$$p_3^2 = \left(-\frac{q}{2} + \frac{1}{6}\sqrt{\frac{D}{3}}\right)^{1/3} + \left(-\frac{q}{2} - \frac{1}{6}\sqrt{\frac{D}{3}}\right)^{1/3} - \frac{b_2}{3b_3}. \qquad \text{(B-3)}$$

To compute the derivative dp_3/dp_1, we differentiate equation (B-1), keeping in mind that $db_3/dp_1 = 0$,

$$6b_3p_3^5\frac{dp_3}{dp_1} + 4b_2p_3^3\frac{dp_3}{dp_1} + 2b_1p_3\frac{dp_3}{dp_1} + p_3^4\frac{db_2}{dp_1} + p_3^2\frac{db_1}{dp_1} + \frac{db_0}{dp_1} = 0. \quad \text{(B-4)}$$

From equation (B-4), we obtain

$$\frac{dp_3}{dp_1} = -\frac{p_3^4\frac{db_2}{dp_1} + p_3^2\frac{db_1}{dp_1} + \frac{db_0}{dp_1}}{2p_3\left(3b_3p_3^4 + 2b_2p_3^2 + b_1\right)}, \quad \text{(B-5)}$$

where p_3 is given in equation (A-3). $3b_3p_3^4 + 2b_2p_3^2 + b_1 \neq 0$ since we do not have singularity points for the VTI medium.

Equations (B-3) and (B-5) can be used in computing offset-traveltime parametric equations (can be computed from parametric equations (27)),

$$\begin{aligned} x(p_1) &= -z\frac{dp_3}{dp_1}, \\ t(p_1) &= zp_3 + xp_1. \end{aligned} \quad \text{(B-6)}$$

Exactly the same equations can be used for SV-wave slowness surface equation (24).

List of Figures

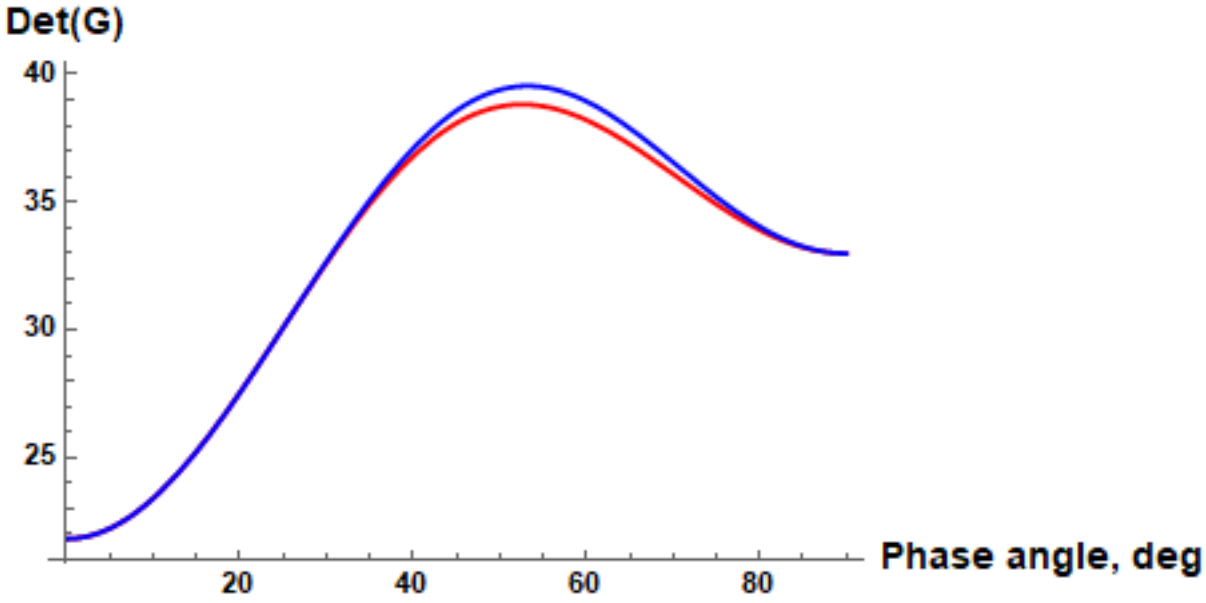

Figure 1. The exact (blue) and approximate, $v_P^2 v_{SV}^2$, (red) determinant of the P-SV block of Christoffel matrix computed for the Green Horn Shale model.

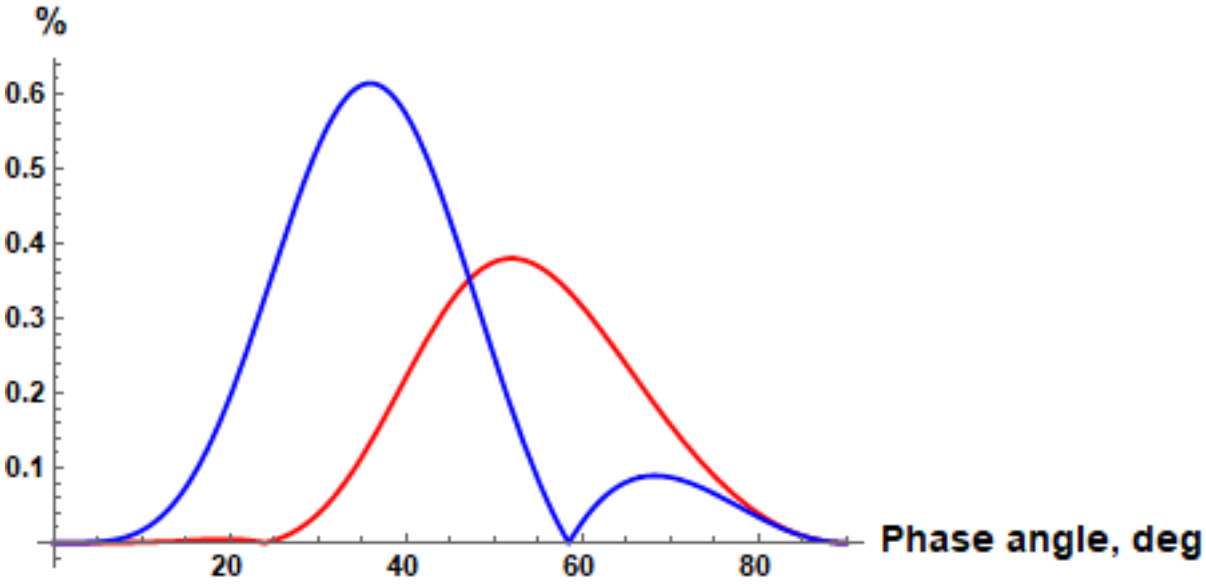

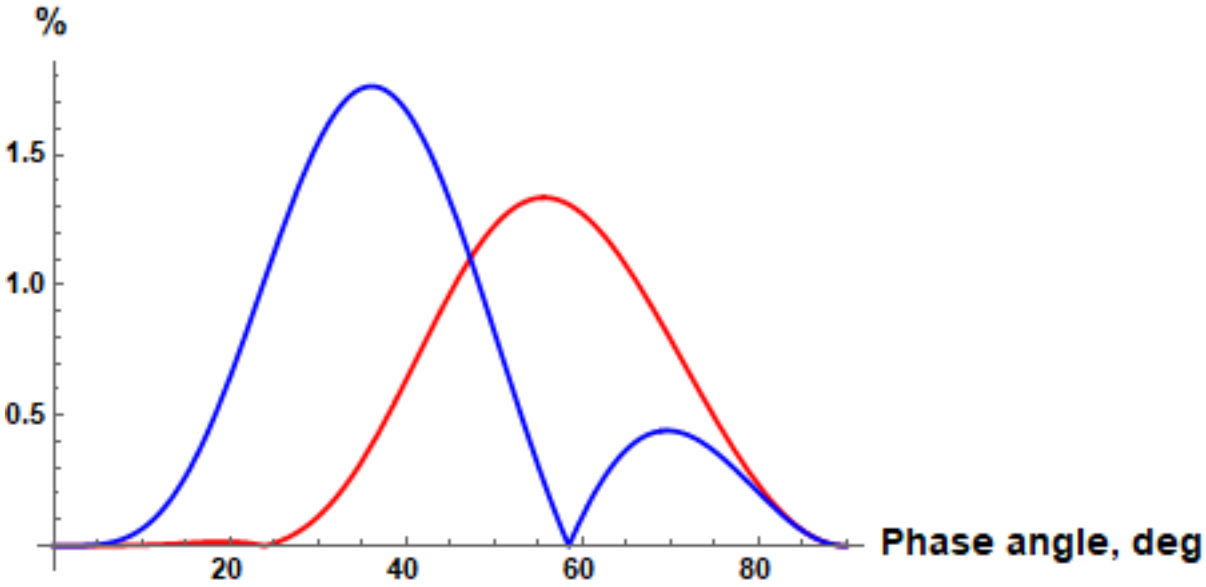

Figure 2. Error in phase velocity for P- (left) and SV- (right) waves for a proposed (red) and Pestana et al. (2012) (blue) approximations computed for Green Horn Shale model.

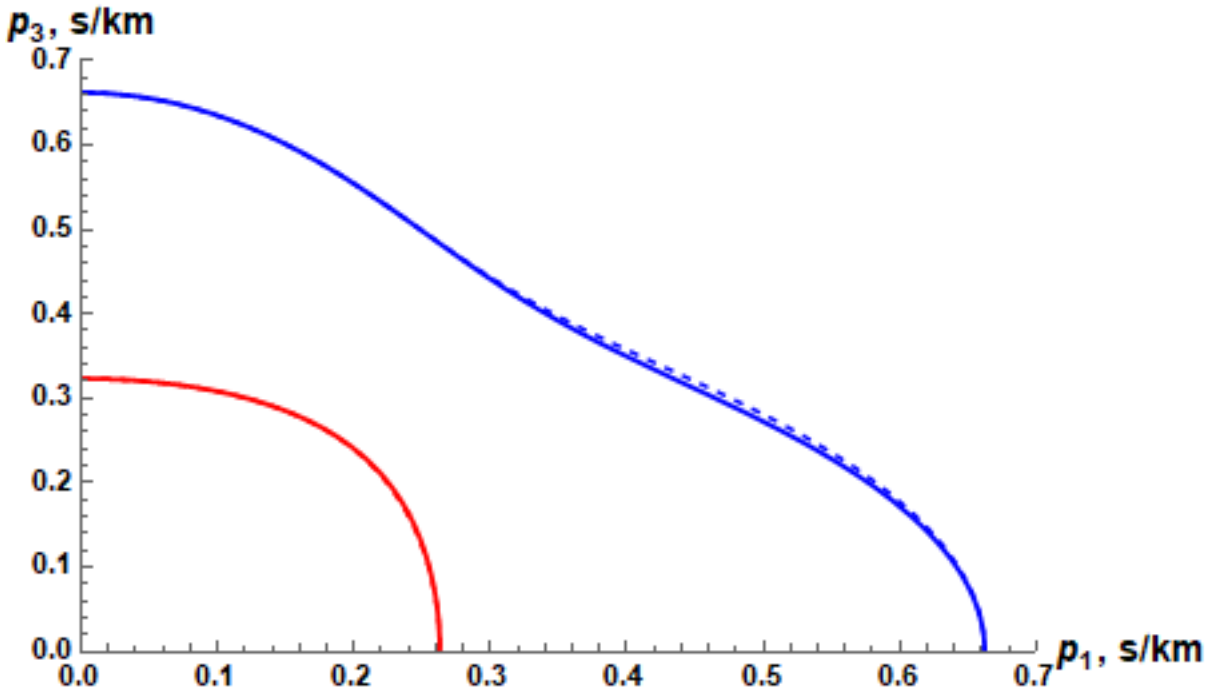

Figure 3. Slowness surface for P- (red) and SV- (blue) waves for proposed approximation (dashed line) and exact equations (blue) computed for Green Horn Shale model.

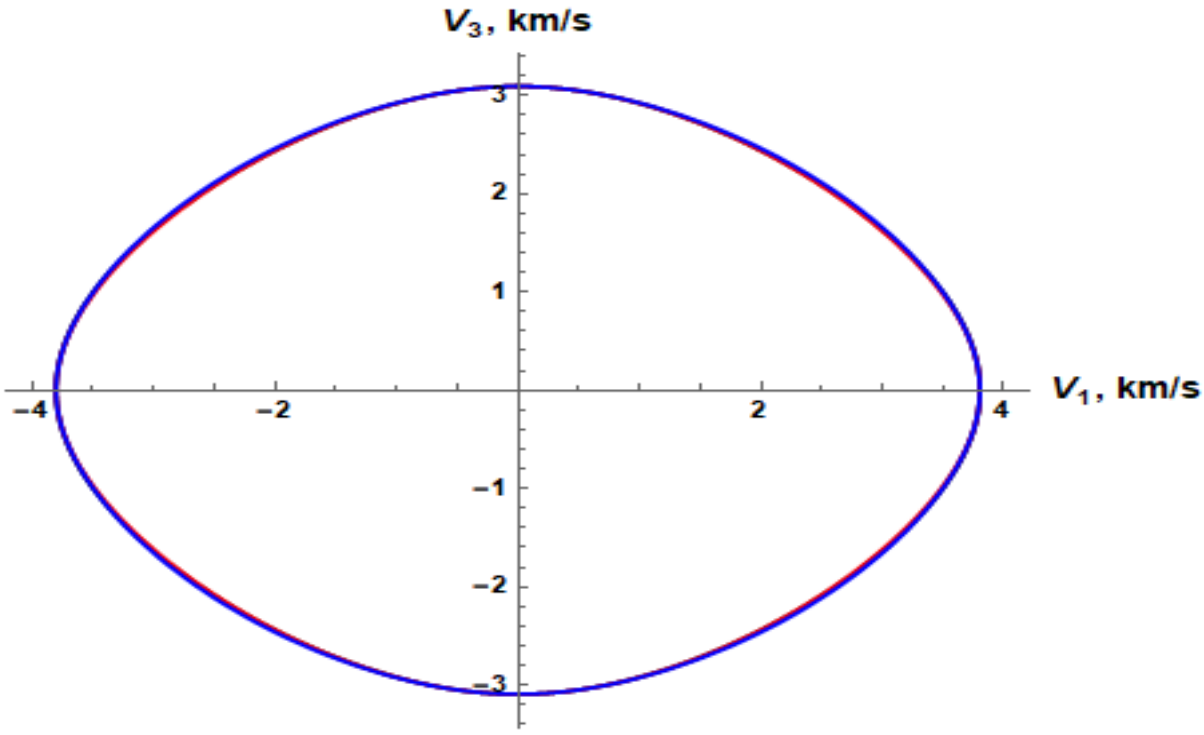

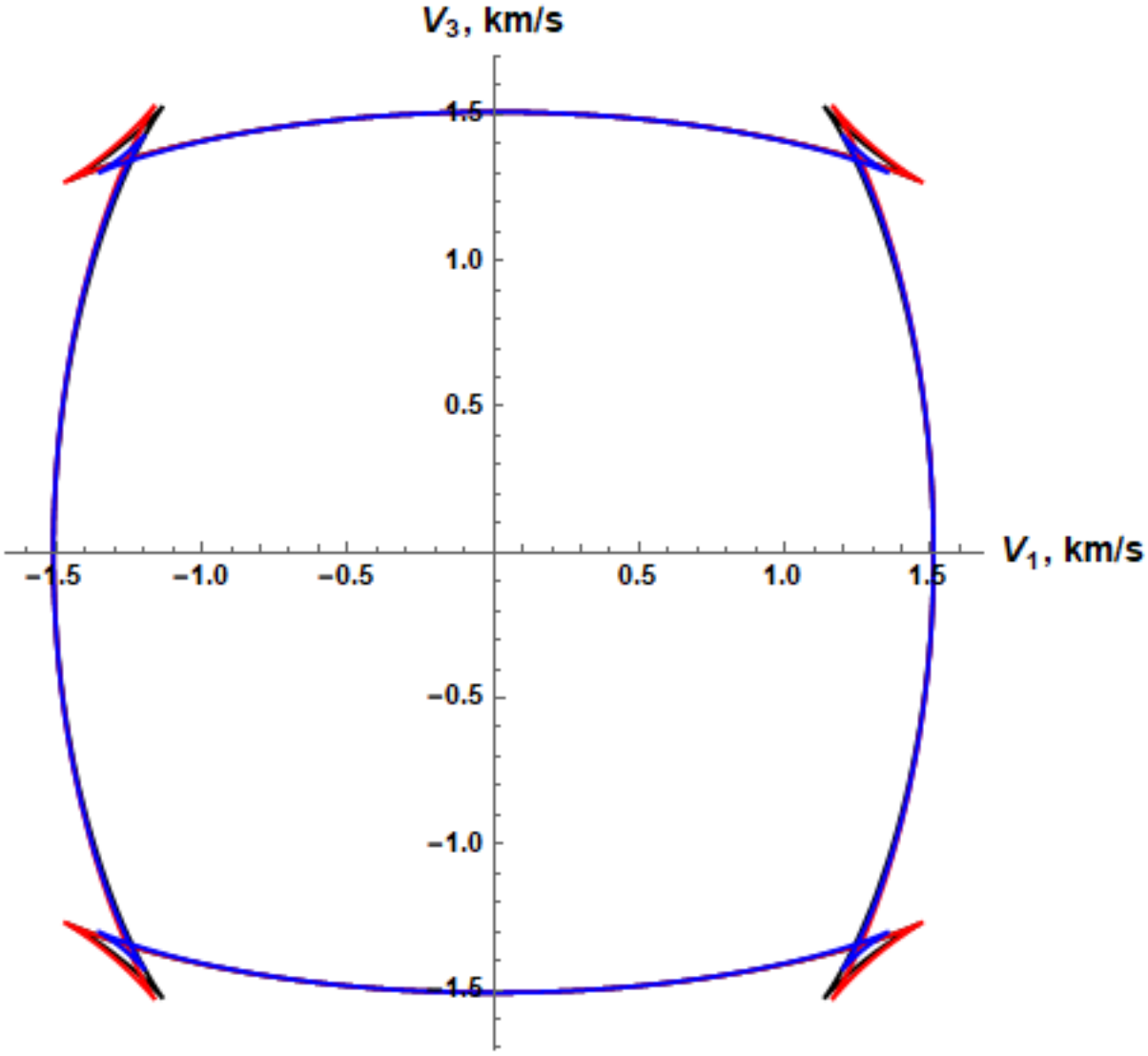

Figure 4. Group velocity surfaces for P- (left) and SV- (right) waves. Elastic solution is shown by black line, proposed and Pestana et al. (2012) approximations are shown by red and blue lines, respectively. The model is Green Horn Shale.

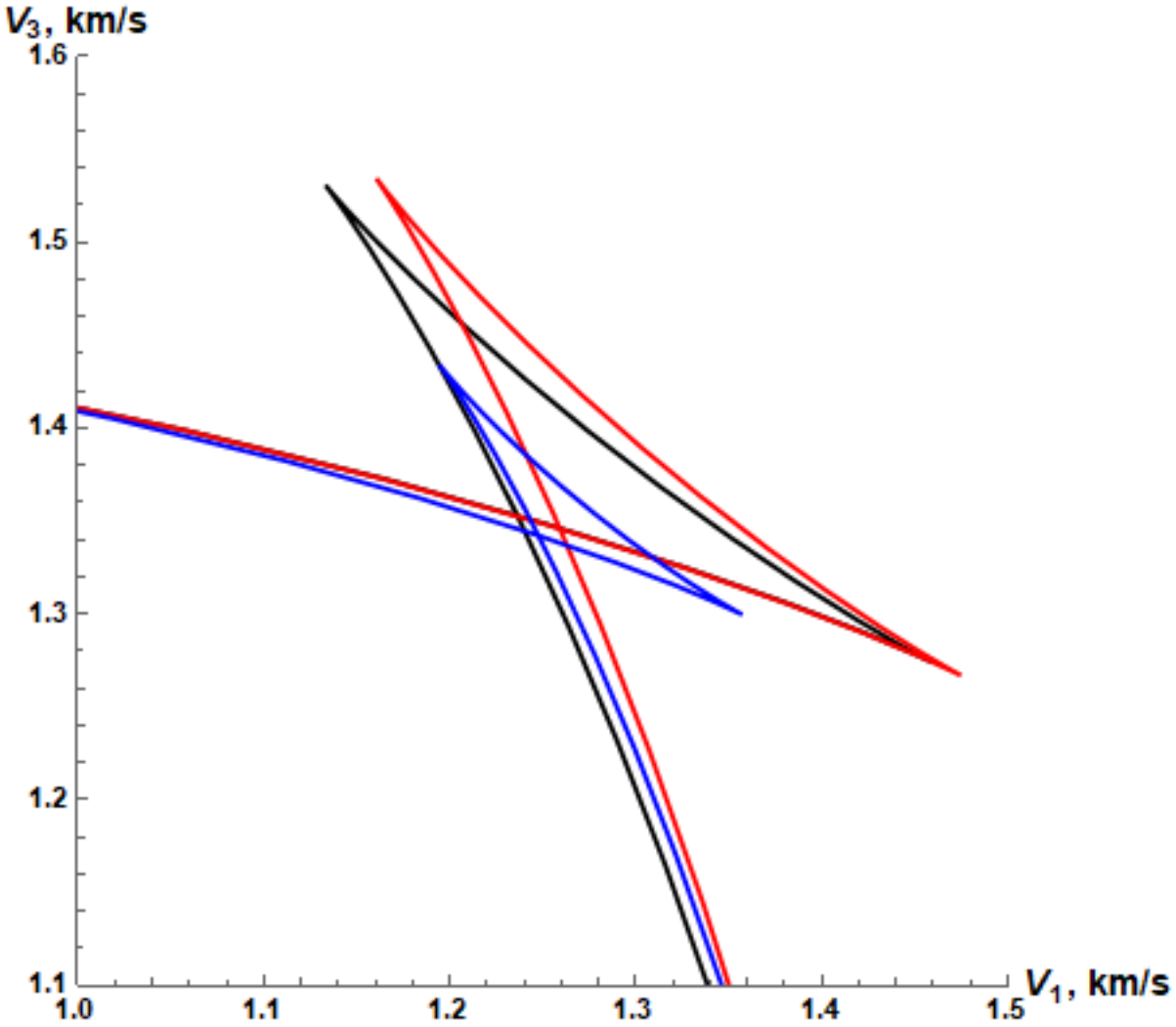

Figure 5. Zoom of SV-wave group velocity surface from Figure 4 to illustrate the triplication. Annotations are the same as for Figure 4.

References

Alkhalifah, T., 1998, Acoustic approximations for processing in transversely isotropic media, *Geophysics*, **63**, no.2, 623-631. https://doi.org/10.1190/1.1444361

Alkhalifah, T., 2000, An acoustic wave equation for anisotropic media, *Geophysics*, **65**, no.2, 1239-1250. https://doi.org/10.1190/1.1444815

Brillouin, L., 1960, Wave propagation and group velocity, Academic Press. https://doi.org/10.1063/1.3057398

Dellinger, J., Muir, F., and Karrenbach, M., 1993, Anelliptic approximations for TI medium, *Journal of Seismic Exploration*, **2**, 23-40. (http://www.geophysical-press.com)

Fowler, P., 2003, Practical VTI approximations: a systematic anatomy, Journal of Applied *Geophysics*, **54**, 347-367. https://doi.org/10.1016/j.jappgeo.2002.12.002

Grechka, V., Zhang, L., and J. W. Rector, 2004, Shear waves in acoustic anisotropic media, *Geophysics*, **69**, no.2, 576-582. https://doi.org/10.1190/1.1707077

Jin, S. and A. Stovas, 2018, S-wave kinematics in acoustic transversely isotropic media with a vertical symmetry axis, *Geophysical Prospecting*, **66**, no.6, 1123-1137. https://doi.org/ 10.1111/1365-2478.12635

Jin, S, and A. Stovas, 2020, S-wave in 2D acoustic transversely isotropic media with a tilted symmetry axis, *Geophysical Prospecting*, **68**, no.2, 483-500. https://doi.org/ 10.1111/1365-2478.12856

Klie, H., and W. Toro, 2001, A new acoustic wave equation for modelling in anisotropic media, SEG expanded abstracts, San Antonio. https://doi.org/10.1190/.1.1816296

Pestana, R.C., Ursin, B., and P. L. Stoffa, 2012, Rapid expansion and pseudo spectral implementation for reverse time migration in VTI media, *JGE*, **9**, no.3, 291-301. https://doi.org/.10.1088/1742-2132/9/3/291

Postnikov, M.M., 1981, Stable polynomials (in Russian), Nauka, Moscow. ISBN 5-354-00637-6

Schleicher, j., and J. Costa, 2016, A separable strong anisotropy approximation for pure qP wave propagation in transversely isotropic media, *Geophysics*, **81**, no.6, C337-C354. https://doi.org/.10.1190/geo2016-0138.1

Schoenberg, M.A., and M.V. de Hoop, 2000, Approximate dispersion relations for qP – qSV -waves in transversely isotropic media, *Geophysics*, **65**, no.3, 919-933. https://doi.org/10.1190/1.1444788

Sripanich Y. and S. Fomel, 2015, On anelliptic approximations for qP velocities in transversely isotropic and orthorhombic media, *Geophysics*, **80**, no.5, C89–C105. https://doi.org/10.1190/geo2014-0534.1

Stopin, A., 2001, Comparison of v(q) equations in TI medium, 9th International Workshop on Seismic Anisotropy. https://doi.org/10.1190/.1.9781560801771.ch20

Stovas, A., and S. Fomel., 2019, Generalized velocity approximation, *Geophysics*, **84**, no.1, C27-C40. https://doi.org/10.1190/geo2018-0401.1

Xu, S., Stovas, A, Alkhalifah, T., and H. Mikada, 2020, New acoustic approximation for transversely isotropic media with a vertical symmetry axis, *Geophysics*, **85**, no.1, C1-C12. https://doi.org/10.1190/geo2019-0100.1

Data Availability Statement: Not applicable.

There is not any conflict of interest.